THEORETICAL & APPLIED MECHANICS LETTERS **4**, 041010 (2014)

Energy barrier for configurational transformation of graphene nanoribbon on nanotube

Qifang Yin, Xinghua Shi[a)]
LNM, Institute of Mechanics, Chinese Academy of Sciences, Beijing 100190, China

(Received 15 April 2014; revised 8 May 2014; accepted 14 May 2014)

Abstract A graphene nanoribbon (GNR) has two basic configurations when winding on the outer surface of a carbon nanotube (CNT): helix and scroll. Here the transformation between the two configurations is studied utilizing molecular dynamics simulations. The energy barrier during the transformation as well as its relationship with the interfacial energy and the radius of CNT are investigated. Our work offers further insights into the formation of desirable helix/scroll of GNR winding on nanotubes or nanowires, and thus can enable novel design of potential graphene-based electronics.

 [doi:10.1063/2.1404110]

Keywords nanoscroll, helix, energy barrier, mechanics of micro/nano structures, molecular dynamics method

The graphene nanoribbons (GNRs) have potential application in future electronic devices due to their tunable band gap.[1–4] The syntheses of GNRs thus attract enormous attention.[5–8] Due to thermal fluctuations, suspended GNRs with high aspect ratio have a tendency to be in complicated grouped states,[9–11] which greatly impedes their applications. Guide the suspended GNRs into regular configurations becomes the key in mass synthesis of GNRs. Carbon nanotube-induced assembly of GNRs is one successful example to promote the thermodynamic stability of GNRs.[12–15] It has been reported that on nanotube, the winded GNRs basically have two stable configurations: helix and scroll (Figs. 1(a) and 1(e)).[12–15] For scroll, it has been reported to play important roles in innovative nano-devices such as nano-oscillator,[16] hydrogen storage,[17] water and ion tunnels,[18] and energy absorption.[19] Numerous approaches to fabricate scroll have thus been proposed,[20–23] and the assembly from GNR is the promising one.[13,14] Through static potential energy calculation, we have revealed in our previous work that the helix or scroll configuration is determined by the tube radius, bending stiffness of GNR, length of GNR, and interfacial energy.[15] However, the transformation between the two configurations remains elusive. From the views of both assembling GNR and synthesizing scroll, it is desirable to further investigate the configurational transformation of GNR on nanotube. In this letter, we have studied the transformation between the two configurations and calculated the energy barrier during the transformation with molecular dynamics (MD) simulations. Our work provides guidance for novel design of potential graphene-based nano-device.

In MD simulations, a series of zigzag carbon nanotube (CNTs) with different radius are constructed. Correspondingly the length of GNR is about $2\pi(r_0+d)+2\pi(r_0+2d)$, where r_0 is the

[a)]Corresponding author. Email: shixh@imech.ac.cn.

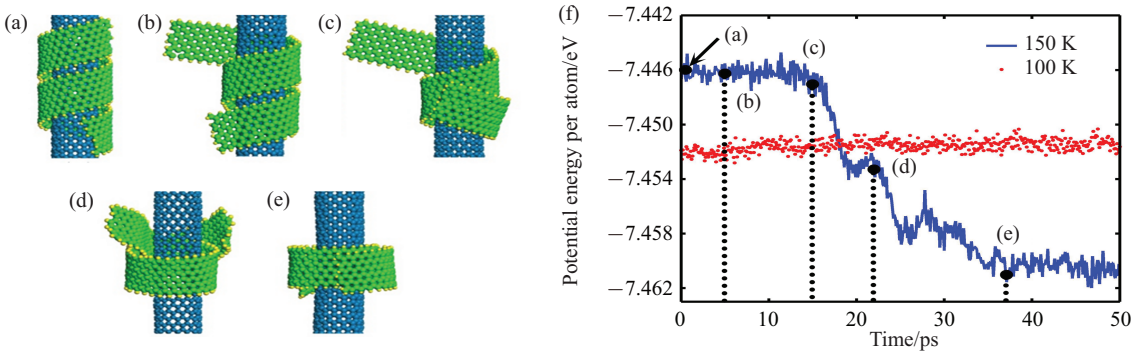

Fig. 1. Plots (a)–(e) are snapshots of transform of a GNR from helix configuration to scroll on a (14, 0) CNT. Plot (f) denotes the total potential energy per atom during this process. The solid line represents a successful transform at 150 K and the dash line for a failed process at 100 K. Labels (a)–(e) are respectively corresponding to the energy state at the time marked on plot (f).

radius of CNT and $d = 0.34$ nm the interlayer space. The width of GNR is 1.256 4 nm. All the dangling bonds in the GNR are passivated with hydrogen atoms to avoid chemical reactions. The C-C and C-H bonds are described by the adaptive intermolecular reactive empirical bond order potential (AIREBO).[24] The interaction between CNT and GNR is described by Lennard–Jones (L–J) potential $E = 4\lambda\varepsilon_{c-c}[(\sigma_{c-c}/r)^{12} - (\sigma_{c-c}/r)^{6}]$, where $\lambda = \varepsilon_{t-g}/\varepsilon_{g-g}$ is a factor tuning the intensity of the interaction,[18] ε_{t-g} is the L–J parameter between the CNT and the GNR, $\varepsilon_{g-g} = \varepsilon_{c-c} = 0.002\,84$ eV is the L–J parameter between GNR itself, and $\sigma_{c-c} = 0.34$ nm. All the MD simulations are performed using LAMMPS packages[25] with microcanonical ensemble (NVE).

To illustrate how the energy barrier prevents the helix transforming into scroll, we first set up a model system where GNR winds on a (14, 0) CNT into a helix structure (Fig. 1(a)). In our previous work we have shown that to maintain a helix structure, energetically the tuning factor λ should be a large value, otherwise the final structure would be a scroll.[15] Here we tune λ to a small one ($\lambda = 0.281$) and run a MD simulation at temperature $T = 100$ K. In a 100 ns run it is seen that the structure keeps being a helix, which is contradictory to our previous finding.[15] This contradiction could be explained by the existence of energy barrier during the transformation from helix to scroll. As we increase the temperature to 150 K, it is seen that the helix structure spontaneously transforms into scroll (Figs. 1(a)–1(e)), which means the energy barrier could be overcome via thermal undulation. The solid line in Fig. 1(f) shows the profile of potential energy of the system for the successful transformation while the dashed one represents a failed one.

Similarly, to demonstrate the existence of energy barrier within the transformation from scroll to helix, we repeat the MD simulations in which initially the GNR winds on the nanotube into a scroll (Fig. 2(a)). This time λ is set to 4.93 and according to the prediction in Ref. 15, the final configuration should be helix. However it is seen that at temperature $T = 300$ K, the configuration keeps being a scroll during a 10 ns MD run (Fig. 2(a)). The structure spontaneously transforms into the helix only when the temperature increases to 400 K. The snapshots of the process are shown in Figs. 2(a)–2(e) and the profiles of potential energy for successful and failed transformations are shown in Fig. 2(f). We conclude that the energy barriers do exist during the

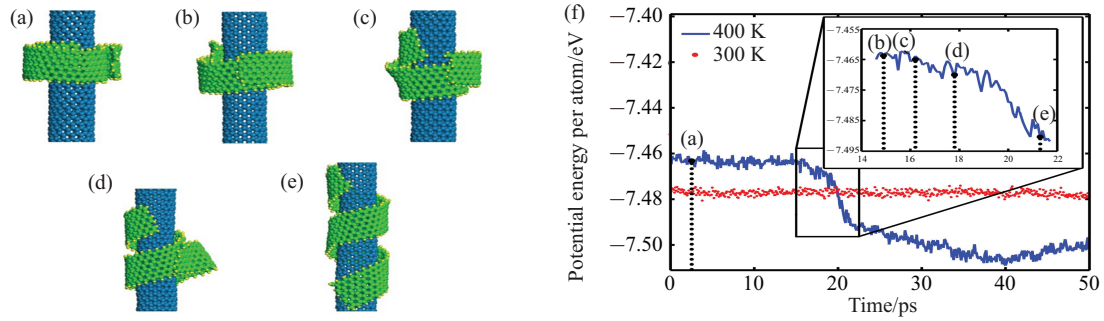

Fig. 2. Plots (a)–(e) are snapshots of transform of GNR from scroll to helix on a (14, 0) CNT. Plot (f) denotes the total potential energy per atom during this process. The solid line means a successful transformation at 400 K and the dash line a failed one at 300 K. Plots (a)–(e) are respectively corresponding to the energy state at the time marked on plot (f).

transformation between the two configurations.

We become interested in how large the energy barrier is and how the geometrical, interfacial parameters quantitatively influence the energy barrier. To answer these questions, we construct a series of zigzag CNTs with different radius ((14, 0), (20, 0), (25, 0), (35, 0), (45, 0)) and conduct a series of MD simulations with λ changed from 0.1 to 1.2. Here the chirality and torsion correlated effects of CNTs and GNR are ignored.[15] The geometric parameters of GNR are the same as those in the above simulations.

In the calculations, a GNR scrolls on CNT at 10 K in NVE ensemble. Then two ends of the GNR are pulled oppositely along the axial direction of CNT. The pulling speed is fixed at 0.01 nm/ps. In this manner, the scroll would be driven into helix configuration. The snapshot of the atoms' coordinates is recorded every 5 ps during the pull. Energy minimization is then performed to each snapshot with conjugate gradient algorithm[24] to eliminate thermal undulations. The minimized potential energy per atom as a function of L, the distance of the two pulled ends, is plotted in Fig. 3 with $\lambda = 0.9$.

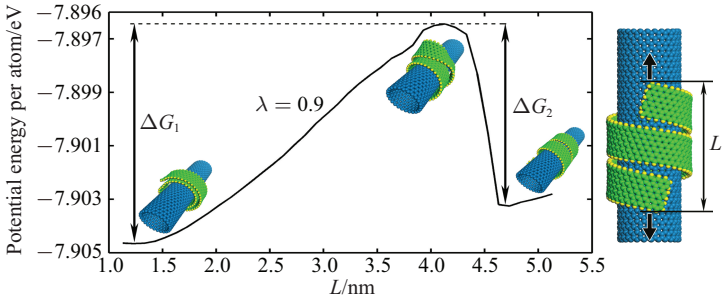

Fig. 3. Minimized potential energy as a function of L with $\lambda = 0.9$ and CNT chirality (25, 0). Insets are the configurations at corresponding conditions.

In the energy profile there are two local minima and one maximum (Fig. 3). The difference between the first minimum and the peak, marked as ΔG_1, is the energy barrier of the transformation from scroll to helix, and the second one ΔG_2 is the energy barrier of the transformation from helix to scroll. ΔG_1 and ΔG_2 are plotted in Fig. 4 as a function of λ which indicates the

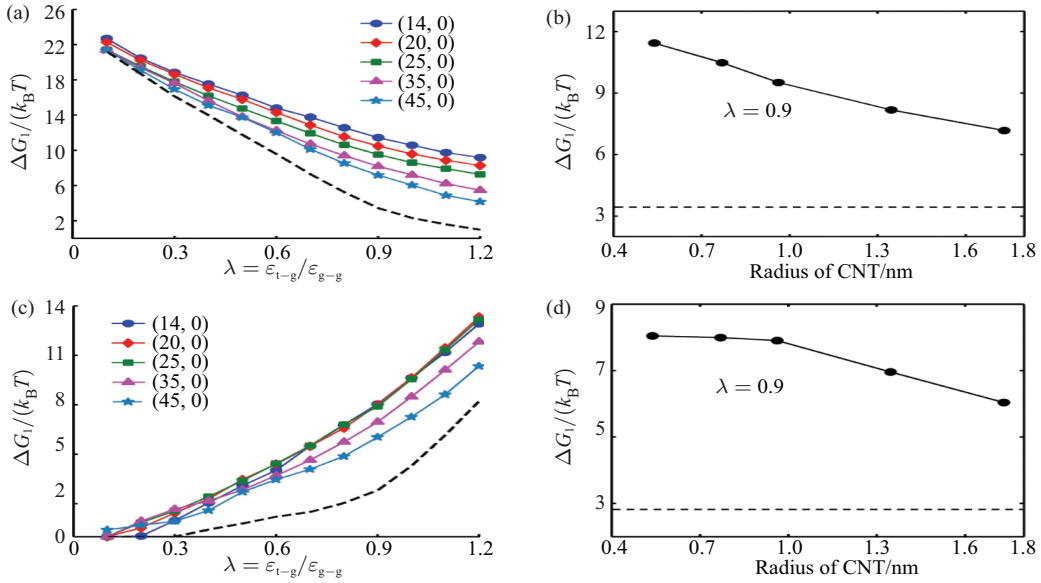

Fig. 4. (Colored online) Relationship of energy barrier ΔG_1 with (a) λ and (b) the radius of CNT, ΔG_2 with (c) λ and (d) the radius of CNT. k_B is the Boltzmann constant and $T = 10$ K is the absolute temperature. The dashed lines in the plots are the cases of an infinite-radius CNT.

intensity of interfacial energy. It is seen that ΔG_1 decreases as λ increases while ΔG_2 increases with λ. Since large λ indicates a strong attraction of GNR toward CNT, rather than roll itself up. So for large λ the energy barrier for transformation from helix to scroll, ΔG_2, becomes large (Fig. 4(c)) while for energy barrier for transformation from scroll to helix, ΔG_1, becomes small (Fig. 4(a)). The size of nanotube can influence the energy barrier as shown in Figs. 4(a) and 4(c): both of them decrease as size of tube increases. The mechanisms, however, are different. For ΔG_1, it is mainly arises from the difference of bending energy when the GNR rolls around itself and around the tube, which is proportional to $1/(r_0+d)^2 - 1/(r_0+2d)^2$. The difference of bending energy decreases as the tube radius r_0 increases, which effectively reduces ΔG_1. For comparison, we plot the profile of energy barrier in an extreme case where the tube is replaced by a plane, indicating the radius of tube is infinitely large (Fig. 4(a), dash line). For ΔG_2, it is mainly due to the difference of interaction energy when GNR rolls around the tube and around itself, which is proportional to $\sigma_{t-g}^6/(r_0+2d)^{12} - 1/(r_0+2d)^6 - \sigma_{t-g}^6/(r_0+d)^{12} + 1/(r_0+d)^6$. The difference of interaction energy decreases as the tube r_0 increases, which also reduces ΔG_2. The dash line in Fig. 4(c) indicates the lower bound of energy barrier when the radius of tube is infinitely large.

Due to the pulling scheme in the forced transformation, the energy barrier for scroll to helix arises from the second innermost ring as it attaches to the tube, so the length of ribbon has no effect to the energy barrier. For the case of helix to scroll, which is an inverse process of scroll to helix, the length of the ribbon has no effect to the energy barrier either.

In summary, we have investigated the energy barrier in the configurational transformation of GNR between helix and scroll. For fixed GNR/GNR interaction, the energy barrier of transformation from scroll to helix decreases as GNR/CNT interaction increases, while the barrier of transformation from helix to scroll increases with GNR/CNT interaction. Both the energy barriers for the two transformations decreases as the radius of tube increases, indicating the large tube

can reduce the energy barrier. Our work offers further insights into the formation of desirable helix/scroll of GNR winding on nanotubes or nanowires, and thus can enable novel design of potential graphene-based electronics.

The work is supported by the National Natural Science Foundation of China (NSFC) (11272327 and 11023001), and computation is mainly supported by the Supercomputing Center of Chinese Academy of Sciences (SCCAS).

1. V. Barone, O. Hod, G. E. Scuseria. Electronic structure and stability of semiconducting graphene nanoribbons. *Nano Lett.* **6**, 2748–2754 (2006).
2. T. B. Martins, R. H. Miwa, A. J. da Silva, et al. Electronic and transport properties of boron-doped graphene nanoribbons. *Phys. Rev. Lett.* **98**, 196803 (2007).
3. X. Wang, Y. Ouyang, X. Li, et al. Room-temperature all-semiconducting sub-10-nm graphene nanoribbon field-effect transistors. *Phys. Rev. Lett.* **100**, 206803 (2008).
4. Z. H. Chen, Y. M. Lin, M. J. Rooks, et al. Graphene nano-ribbon electronics. *Physica E.* **40**, 228–232 (2007).
5. A. Chuvilin, E. Bichoutskaia, M. C. Gimenez-Lopez, et al. Self-assembly of a sulphur-terminated graphene nanoribbon within a single-walled carbon nanotube. *Nat. Mater.* **10**, 687–692 (2011).
6. L. Jiao, L. Zhang, X. Wang, et al. Narrow graphene nanoribbons from carbon nanotubes. *Nature* **458**, 877–880 (2009).
7. X. Li, X. Wang, L. Zhang, et al. Chemically derived, ultrasmooth graphene nanoribbon semiconductors. *Science* **319**, 1229–1232 (2008).
8. L. Ci, Z. P. Xu, L. L. Wang, et al. Controlled nanocutting of graphene. *Nano Res.* **1**, 116–122 (2008).
9. Z. Xu, M. J. Buehler. Geometry controls conformation of graphene sheets: membranes, ribbons, and scrolls. *ACS Nano* **4**, 3869–3876 (2010).
10. B. V. Martins, D. S. Galvao. Curved graphene nanoribbons: structure and dynamics of carbon nanobelts. *Nanotechnology* **21**, 75710 (2010).
11. A. L. J. Pang, V. Sorkin, Y. W. Zhang, et al. Self-assembly of free-standing graphene nano-ribbons. *Phys. Lett. A* **376**, 973–977 (2012).
12. Y. Jiang, H. Li, Y. Li, et al. Helical encapsulation of graphene nanoribbon into carbon nanotube. *ACS Nano* **5**, 2126–2133 (2011).
13. N. Patra, Y. Song, P. Kral. Self-assembly of graphene nanostructures on nanotubes. *ACS Nano* **5**, 1798–1804 (2011).
14. Z. Zhang, T. Li. Carbon nanotube initiated formation of carbon nanoscrolls. *Appl. Phys. Lett.* **97**, 081909 (2010).
15. Q. Yin, X. Shi. Mechanics of rolling of nanoribbon on tube and sphere. *Nanoscale* **5**, 5450–5455 (2013).
16. X. H. Shi, Y. Cheng, N. M. Pugno, et al. A translational nanoactuator based on carbon nanoscrolls on substrates. *Appl. Phys. Lett.* **96**, 053115 (2010).
17. S. F. Braga, V. R. Coluci, R. H. Baughman, et al. Hydrogen storage in carbon nanoscrolls: An atomistic molecular dynamics study. *Chem. Phys. Lett.* **441**, 78–82 (2007).
18. X. Shi, Y. Cheng, N. M. Pugno, et al. Tunable water channels with carbon nanoscrolls. *Small* **6**, 739–744 (2010).
19. X. Shi, Q. Yin, N. M. Pugno, et al. Tunable mechanical behavior of carbon nanoscroll crystals under uniaxial lateral compression. *Journal of Applied Mechanics* **81**, 1014 (2013).
20. M. V. Savoskin, V. N. Mochalin, A. P. Yaroshenko, et al. Carbon nanoscrolls produced from acceptor-type graphite intercalation compounds. *Carbon* **45**, 2797–2800 (2007).
21. X. Xie, L. Ju, X. Feng, et al. Controlled fabrication of high-quality carbon nanoscrolls from monolayer graphene. *Nano Lett.* **9**, 2565–2570 (2009).
22. L. M. Viculis, J. J. Mack, R. B. Kaner. A chemical route to carbon nanoscrolls. *Science* **299**, 1361 (2003).
23. D. Xia, Q. Xue, J. Xie, et al. Fabrication of carbon nanoscrolls from monolayer graphene. *Small* **6**, 2010–2019 (2010).
24. S. Plimpton. Fast parallel algorithms for short-range molecular-dynamics. *Journal of Computational Physics* **117**, 1–19 (1995).
25. D. W. Brenner, O. A. Shenderova, J. A. Harrison, et al. A second-generation reactive empirical bond order (REBO) potential energy expression for hydrocarbons. *Journal of Physics-Condensed Matter* **14**, 783–802 (2002).